Early Prediction of Pharmaceutical Oxidation Pathways by Computational Chemistry and Forced Degradation

Darren L. Reid,[1] C. Jeffrey Calvitt,[1] Mark T. Zell,[1] Kenneth G. Miller,[1] and Carol A. Kingsmill[1,2]

Received February 9, 2004; accepted May 11, 2004

Purpose. To show, using a model study, how electronic structure theory can be applied in combination with LC/UV/MS/MS for the prediction and identification of oxidative degradants.

Methods. The benzyloxazole **1**, was used to represent an active pharmaceutical ingredient for oxidative forced degradation studies. Bond dissociation energies (BDEs) calculated at the B3LYP/6-311+G(d,p)//B3LYP/6-31G(d) level with isodesmic corrections were used to predict sites of autoxidation. In addition, frontier molecular orbital (FMO) theory at the Hartree-Fock level was used to predict sites of peroxide oxidation and electron transfer. Compound **1** was then subjected to autoxidation and H_2O_2 forced degradation as well as formal stability conditions. Samples were analyzed by LC/UV/MS/MS and degradation products proposed.

Results. The computational BDEs and FMO analysis of **1** was consistent with the LC/UV/MS/MS data and allowed for structural proposals, which were confirmed by LC/MS/NMR. The autoxidation conditions yielded a number of degradants not observed under peroxide degradation while formal stability conditions gave both peroxide and autoxidation degradants.

Conclusions. Electronic structure methods were successfully applied in combination with LC/UV/MS/MS to predict degradation pathways and assist in spectral identification. The degradation and excipient stability studies highlight the importance of including both peroxide and autoxidation conditions in forced degradation studies.

KEY WORDS: forced degradation; oxidation; mass spectrometry; computational; pharmaceutical

INTRODUCTION

The benefits of evaluating drug candidates for their oxidative stability are well recognized by the pharmaceutical industry (1). Since oxidation is probably second only to hydrolysis as a mode of decomposition (2), it is important that analytical methodology be evaluated for its selectivity to oxidative degradants (3). For this reason oxidative stress testing of drug substance is recommended by the International Conference on Harminisation (ICH) and the Food and Drug Administration (FDA) guidelines (4,5). Significant benefits can also be derived if forced degradation studies are used as an opportunity to understand a drug's oxidative stability since the formulation approaches used to control degradation depends on the mechanism of oxidation (6,7). Unfortunately, early identification of the degradation pathways can involve an expense that is not justified at early stages of drug development. Liquid Chromatography/Mass Spectrometry (LC/MS) offers a partial solution and has achieved widespread use in the pharmaceutical industry as a method of analysis for stress testing (1). Modern LC/MS methods often require very little additional time over other LC methods and yield considerable information based on the masses of parent and daughter ions. The difficulty in oxidative degradation studies is that many different products can have the same mass (i.e., M + 16 or M + 32). It would be useful if these products could be easily discriminated. A number of approaches have been suggested to supplement information from active pharmaceutical ingredient (API) oxidative forced degradation studies (6,8). These include: cyclic voltammetry/columbic arrays, to determine an API's oxidation potential; and comparison of C-H bond-dissociation energies (BDEs) to experimental models, to determine potential for autoxidation. By their nature, oxidation reactions also lend themselves to a number of simple computational approaches. Although oxidation reactions generally fall under kinetic control, reliable predictions of degradation pathways can be made without fully investigating the transition state by taking advantage of frontier molecular orbital (FMO) theory and bond dissociation energies (BDEs).

Pharmaceutical oxidation can occur by a variety of mechanisms, which can be grouped into three categories: nucleophilic/electrophilic processes, electron transfer processes, and hydrogen atom abstractions. Nucleophilic/electrophilic processes typically occur in the presence of peroxides and can involve nucleophilic attack of peroxide anions under alkaline conditions, or more commonly nucleophilic drugs react with peroxides displacing an alkoxide (6,7). Selectivity of nucleophilic/electrophilic processes of this type can be understood in terms of FMO theory. To a first approximation the key interactions in a nucleophilic attack will be between the highest occupied molecular orbital (HOMO) of the nucleophile (i.e., the lone pair of an amine), and the lowest unoccupied molecular orbital (LUMO) of the electrophile (i.e., the O–O anti-bonding σ*-orbital of a peroxide). Therefore, the HOMO of an API is an indicator of the regiochemistry of peroxide oxidation. HOMOs can reliably be obtained at relatively low levels of theory allowing for the computation of large systems, typical of APIs (9). HOMOs also provide useful information about electron transfer processes, which involve electron transfer from a low electron affinity donor to an oxidizing species. The oxidizing species could be O_2 itself in the presence of catalyzing metals, as in the oxidation of amines to imines. Since from Koopmans' Theorem ($I_i = -e_i$) the ionization enthalpy is equal to the negative of an orbital's energy, the HOMO will indicate the most susceptible site to oxidation by electron transfer. Autoxidation-chain processes represent the third set of reactions of interest. The process is initiated by H-atom abstraction from a weak bond and propagated by subsequent H-abstractions by the resulting peroxyl radicals (6,7). As a consequence of the Hammond postulate, the site of radical formation is determined in large part by the BDE of the X–H bond when the attacking radicals are the same or similar (10,11). As a result, the relative BDEs of the X–H bonds are indicators of the primary site(s) of autoxidation. Accurate BDEs have been difficult to achieve until recently; however, isodesmic methods used in combination with

[1] Analytical Research and Development, Pharmaceutical Sciences, Pfizer Global Research and Development, Ann Arbor, Michigan, 48105, USA.

[2] To whom correspondence should be addressed. (e-mail: Carol.Kingsmill@pfizer.com)

density functional theory now allow for the calculation of BDEs with errors typically less than ±2.5 kcal mol^{-1} (12).

In this work we consider the oxidation of (S)-3-[4-[2-(5-methyl-2-phenyloxazol-4-yl)ethoxy]phenyl]-2-pyrrol-1-yl-propionic acid (13), **1**, (Fig. 1) as an example of how computational chemistry can be applied to the analysis of oxidative forced degradation. Figure 1 indicates that all of the C–H bonds may be susceptible to H-abstraction, while each aromatic ring could be subject to electron transfer, and both the pyrrole and oxazole rings could act as nucleophiles in reactions with peroxides. FMOs from Hartree-Fock calculations and BDEs from Density Functional calculations were used in combination with LC/MS to evaluate the oxidative degradation of **1**. LC/MS/NMR was used to confirm the computational/LC/MS predictions.

MATERIALS AND METHODS

Theoretical Procedures

Frontier Molecular Orbitals

Ab initio calculations were performed using the Spartan'02 Windows molecular modeling package (14). Representative geometries of **1** for determination of the FMOs were located using the conformational Monte Carlo search algorithm with the Merck Molecular Force Field to generate 100 optimized conformations. Seven of these, within 2 kcal mol^{-1} of the lowest energy conformation, were further optimized at the Hartree-Fock level of theory with the 3-21G* basis set. The final HOMO was obtained from a HF/6-31G* single point calculation on the lowest energy HF/3-21G* conformation.

Bond Dissociation Energies

Compound **1** is too large for the level of theory required for accurate determination of BDEs; therefore, the structure was broken down into four smaller representative components: Model 1, (**M1**); Model 2, (**M2**); Model 3, (**M3**); and

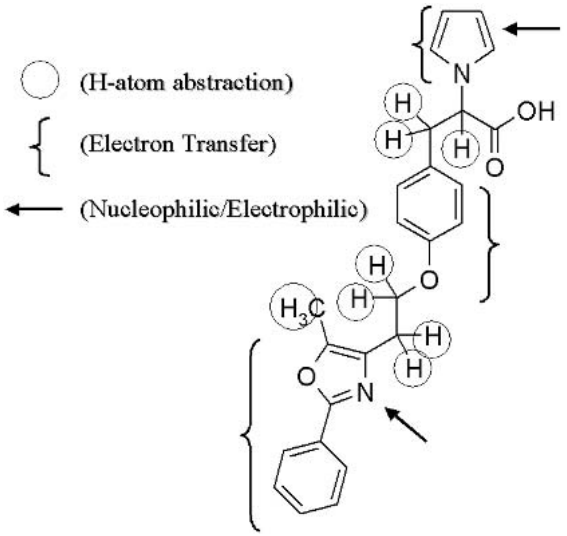

Fig. 1. Possible sites of oxidative reactivity for **1**.

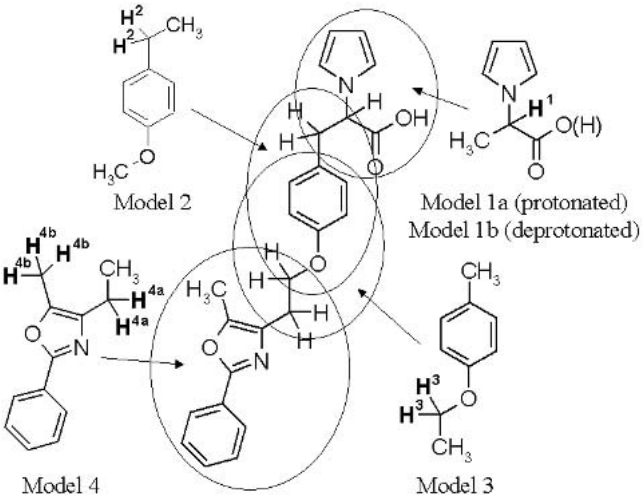

Fig. 2. Representative models of compound **1** for the BDE study showing hydrogen atoms at abstraction sites in bold.

Model 4, (**M4**) as shown in Fig. 2. A corresponding numbering system for the hydrogens is also presented in Fig. 2. The parent structure was divided at points at least one σ-bond away from the H-abstraction site so that no potential π-system was removed from conjugation with a radical site. Geometry optimizations and frequency calculations were carried out using the B3LYP hybrid HF-DFT implemented in Spartan'02 with the 6-31G(d) basis set followed by single-point calculations at the 6-311 + G(d,p) level. Frequencies were scaled by a factor of 0.98 in the calculation of the zero point energy (ZPE) corrections, and the thermodynamic function, H_{corr} (15). Basis set superposition error is known to be relatively small (~0.25 kcal mol^{-1}) for the B3LYP functional with large basis sets similar to the one used here, therefore a correction has not been applied (16).

Bond Dissociation Energies at 298 K

The C-H bond dissociation enthalpy (BDE) for the **M1** is defined as the heat of reaction (Eq. (1)), D_{CH}(**M1**) (= $\Delta H_{(1)}^{\circ}$). If calculated directly D_{CH} for amino acid derivatives is subject to substantial computational error, due to basis set and correlation effects, being calculated to be ~8 kcal mol^{-1} too low at the present theoretical level.

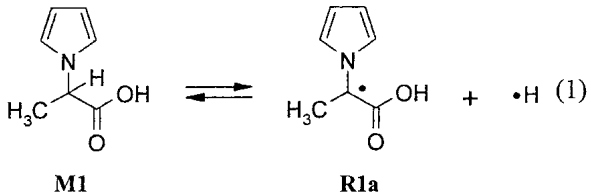

In order to reduce the affects of these errors on the calculated heats of reaction, the BDEs were derived from the heats of isodesmic reactions (17). Here, reaction 1 was used with H_2NCH_2COOH (D_{CH}(**AH**) = 79.11 kcal mol^{-1}) (18) as the reference molecule, **AH**.

$$\mathbf{R1a}^{\bullet} + \mathbf{AH} \rightleftharpoons \mathbf{M1} + \mathbf{A}^{\bullet} \quad (2)$$

Table I. Total Energies, Zero Point Corrections, Experimental Corrections, Temperature Corrections to the Enthalpies, and Bond Dissociation Energies for Each Species

	B3LYP/6-31G(d)			B3LYP/6-311+G(d,p)// B3LYP/6-31G(d)		
Species	Energy hartrees	ZPE kcal mol^{-1}	H_{corr} kcal mol^{-1}	Energy hartrees	ΔD kcal mol^{-1}	BDE kcal mol^{-1}
Stable species						
Toluene	–271.566690	78.95	3.92	–271.638741	3.54	—
Propylene	–117.907543	49.22	2.59	–117.945519	4.70	—
Methanol	–115.714408	31.68	2.06	–115.764801	2.98	—
Glycine	–284.423448	49.28	3.54	–284.523963	8.10	—
Model 1a	–477.355822	94.88	6.03	–477.501968	—	85.8
Model 1b	–476.798211	86.54	5.84	–476.960033	—	85.8
Model 2	–425.402468	117.08	6.25	–425.518375	—	86.4
Model 3	–386.090671	99.75	5.24	–386.197192	—	99.0
Model 4	–595.095924	138.13	8.12	–595.250034	—	87.9,* 92.0†
Radicals						
$^{\bullet}$H	–0.500273	0.00	0.889‡	–0.502156	—	—
$^{\bullet}CH_2Ph$	–270.915156	70.65	3.64	–270.987151	—	—
$^{\bullet}CH_2CH=CH_2$	–117.260374	40.82	2.42	–117.298229	—	—
$^{\bullet}CH_2OH$	–115.052037	23.08	2.06	–115.102264	—	—
$^{\alpha}$C-glycyl radical	–283.790367	41.21	3.39	–283.896971	—	—
Radical 1a	–476.720866	85.33	7.57	–476.864590	—	—
Radical 1b	–476.155478	78.34	5.72	–476.314201	—	—
Radical 2	–424.756192	108.14	6.45	–424.871660	—	—
Radical 3	–385.430208	90.92	5.35	–385.529486	—	—
Radical 4a	–594.449597	129.41	8.16	–594.602952	—	—
Radical 4b	–594.452016	129.78	7.87	–594.596468	—	—

* BDE for C-H^{4a} bond.
† BDE for C-H^{4b} bond.
‡ Translational enthalpy.

Then one has:

$$D_{CH}(\mathbf{M1}) = D_{CH}(\mathbf{AH}) - \Delta H_{(2)}^{\circ} \quad (3)$$

where $\Delta H_{(2)}^{\circ}$ was calculated from the energies of the four species in Eq. 2 each computed at the B3LYP/6-311 + G(d,p)//B3LYP/6-31 + G(d,p) level of theory. This procedure has been shown to yield D_{CH}(**M1**) values with an accuracy within 2.5 kcal mol^{-1} (18,19). The difference in BDE between the best value (isodesmic or from experiment) and the directly calculated value, $\Delta D_{CH}(\mathbf{AH})$ = 8.10 kcal mol^{-1}, is attributed primarily to $\mathbf{A}^{\bullet}$. In a parallel manner, ΔD_{CH} values for benzyl radical, allyl radical and $^{\bullet}CH_2OH$ are given in Table I and may be derived from the experimental BDEs of the parent species (20–28).

Thermochemical Procedures

Thermochemistry The values of thermal enthalpies, $H_{(corr)}$, required to obtain heats of reaction at 298 K were

Table II. Conditions for Oxidative Degradation and Excipient Blend Experiments

Condition	Compound **1** conc.	Time-points	Temp.	Diluent
Autoxidation				
1) Pressurized O_2 without ACVA	1 mg/ml	Day 1, day 5, day 10	60°C	40/60: H_2O/CH_3CN
2) Pressurized O_2 with 5 mol% ACVA	1 mg/ml	Day 1, day 5, day 10	60°C	40/60: H_2O/CH_3CN
3) ATM O_2 with 5 mol% ACVA	1 mg/ml	Day 1, day 5, day 10	60°C	40/60: H_2O/CH_3CN
Nucleophilic/electrophilic oxidation				
4) Hydrogen peroxide	1 mg/ml	Day 1, day 5, day 10	RT	40/60: 6% H_2O_2/CH_3CN
Excipient blend				
5) ATM O_2	4%	6 weeks	RT	—
5) ATM O_2	4%	6 weeks	60°C	—
6) Pressurized O_2	4%	6 weeks	60°C	—
7) 75% relative humidity	4%	6 weeks	40°C	—

calculated by standard statistical thermodynamic methods, based on the rigid rotor-harmonic oscillator model using Spartan'02 (29). All torsional motions were treated as vibrations.

Enthalpy H $(= H^{\circ}_{298K})$ Experimentally, the equation for enthalpies of reaction $(\Delta_r H^{\circ}_{298K})$ requires taking the appropriate sums and differences of the heats of formation $(\Delta_f H^{\circ}_{298K})$ for the reactants and products. Since Spartan'02 provides the thermal enthalpy corrections for molecules $(H_{(corr)})$, and the atomic enthalpy contributions cancel, the enthalpies of reaction are equal to the difference of the sums of $E_{BO} + H_{corr}$ for reactants and products (Eq. 4) (30).

$$\Delta_r H^{\circ}_{298\,K} = \sum_{products} (E_{BO} + H_{corr}) - \sum_{reactants} (E_{BO} + H_{corr}) \qquad (4)$$

Experimental Procedures

Materials

Microcrystalline Cellulose (MCC, Avicel PH 102) supplied by FMC. Dicalcium Dihydrate (DiTAB) supplied by Rhodia. Crospovidone supplied by ISP. Povidone (Kollidon 30) supplied by BASF. Reagents and HPLC-grade solvents (Mallinckrodt, Phillipsburg, NJ) were used without further purfication.

HPLC Conditions

Chromatographic separations for LC/MS analysis were performed on an Agilent 1100 HPLC (Agilent Technologies, Wilmington, DE). For isocratic separations of forced degradation samples three microliter injections were chromatographed using a 100 mm × 2 mm, 120 Å YMC Pro C18, S-3 μm column. The pump was run at 0.25 ml/min with a mobile phase consisting of 65:35:0.2 CH_3CN:H_2O:acetic acid. Excipient samples were separated using a 150 mm × 4.6 cm, YMC-PackPro C-18, S-3μm column under gradient conditions (90:10:0.2 to 10:90:0.2 H_2O:CH_3CN:acetic acid over 25 min with an isocratic hold until 35 min).

Mass Spectrometry Conditions

All LC/MS and LC/MS/MS experiments were performed using a Quattro Micro triple quadrupole electrospray ionization mass analyzer (Micromass, Beverly, MA). Capillary voltage, source temperature, and desolvation temperature were constant in all experiments at 3.5 kV, 120°C, and 350°C respectively. Full scan MS data was acquired from 100 to 600 amu over 1 s with an interscan delay of 0.02 s. All LC/MS/MS data was acquired using daughter ion scans, with argon collision gas. Figure 5 details the optimized cone voltages and collision energies for each component.

LC/MS/NMR

All NMR data was acquired on a Varian (Palo Alto, CA, USA) Inova 600 MHz NMR spectrometer equipped with a $^1H[^{13}C]$ pulse field gradient indirect detection microflow LC/NMR probe (60 μl flow cell). Reverse-phase HPLC was carried out on a Varian modular HPLC system, comprised of a Varian 310 pump, Varian Microsorb MV C_{18} column (150 ×

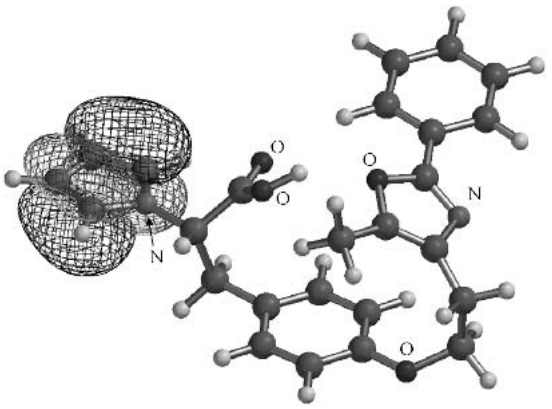

Fig. 3. HOMO of compound 1.

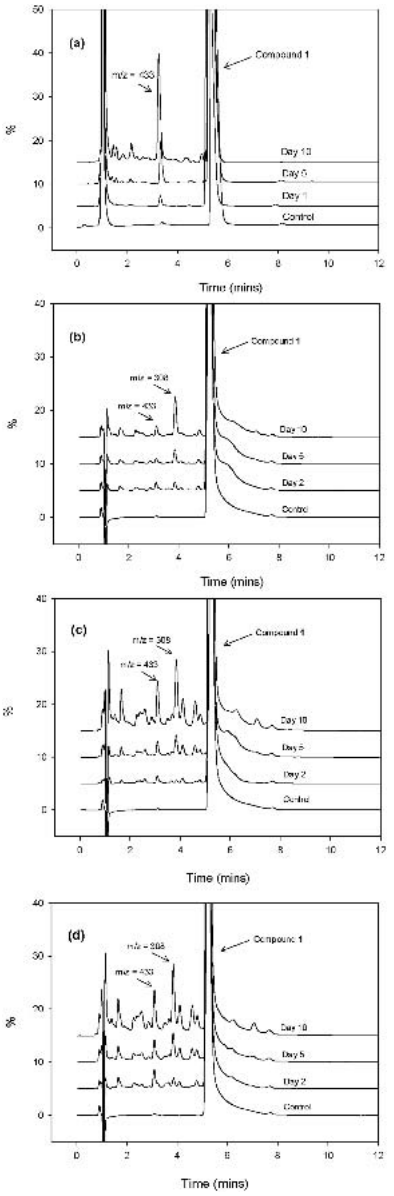

Fig. 4. UV Chromatograms at 220 nm for the oxidation of **1** under autoxidation forced degradation conditions: (a) Hydrogen peroxide oxidation forced degradation conditions; (b) Atmospheric oxygen with initiator at 60°C; (c) Pressurized oxygen without initiator at 60°C; (d) Pressurized oxygen with initiator at 60°C.

4.5 mm I.D.; 5 μm), Varian 9050 UV detector connected in series with a Varian 1200L triple quadrupole MS, and a Varian 210 solvent delivery system pumping 300 μl/min. H_2O/CH_3CN 1:1 make-up solvent to be mixed with eluant flow to the MS. The eluant was monitored by UV (210nm) and MS (scanning 100–500 amu). The flow-rate was 1.0 ml/min. with a post-UV detector splitter delivering 950 μl/min. to the NMR flow probe and 50 μl/min. to the MS. Samples were eluted under gradient conditions (65:35:0.1 to 35:65:0.1 D_2O:CH_3CN:formic acid-d_2 over 12 min, with an isocratic hold until 20 min). Suppression of CH_3CN and HOD signals from the HPLC mobile phase was accomplished by use of the WET pulse sequence (31). NMR spectra were referenced to the CH_3CN solvent signal at 1.94 ppm. For phase sensitive gradient TOCSY spectra a MLEV-17 spin lock with a mixing time of 70 ms was used. A 1 s relaxation delay was used for the acquisition of all spectra.

Oxidative Degradation

Autoxidation and Nucleophilic/electrophilic Conditions

Oxidative degradation conditions for compound **1** were modeled using four sets of experiments: 1) pressurized O_2 without radical initiator; 2) pressurized O_2 with radical initiator; 3) atmosphere with radical initiator; and 4) hydrogen peroxide at room temperature (Table II) (2 ml solution/sample time point). 4,4'-Azobis-(4-cyanovaleric acid) (ACVA) (35 mg/ml) in methanol was used as the radical initiator and O_2 samples were pressurized to 150 psi with O_2 using a Parr general purpose pressure vessel with gage block assembly. Initiator samples were removed at the appropriate time points and quenched with (10 mol%) of an antioxidant solution of ascorbic acid (10 mg/ml) in water. After the day 5 pull, an additional 5 mol% of initiator was added to the atmosphere and pressurized oxygen samples. Before analysis all samples were diluted to 5 ml with acetonitrile.

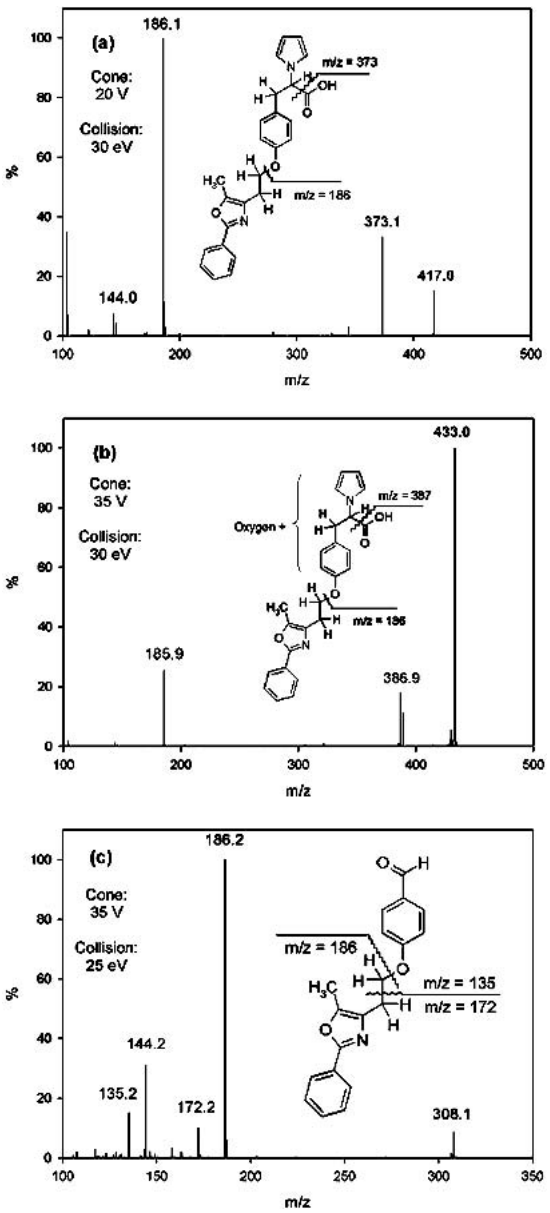

Fig. 5. Collision spectra and proposed fragmentation patterns for (a) compound **1**; (b) degradant **2**; and (c) degradant **3**.

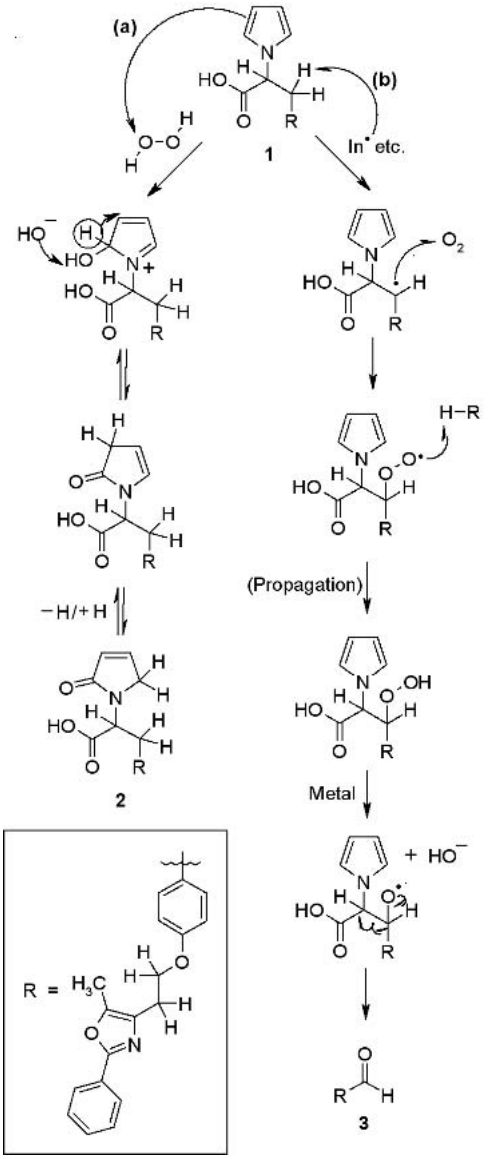

Fig. 6. Proposed mechanisms for formation of: (a) degradant **2**, under peroxide conditions; and (b) degradant **3**, under autoxidation conditions.

Excipient Blend Drug product oxidative degradation conditions of **1** were modeled using an excipient blend consisting of: compound **1**, 4%; Mg-stearate, 1%; microcrystalline cellulose, 42%; dicalcium dihydrate, 42%; crospovidone, 5%; and povidone, 6% (200 mg/sample time point). Two of these excipients, crospovidone and povidone are known sources of peroxide impurities (6,32). Four sets of experimental conditions were tested on 6 weeks stability: atmosphere at R.T., atmosphere at 60°C, pressurized O_2 at 60°C and 40°C/75% relative humidity (Table II). Before analysis 10 ml of H_2O was added to each sample and brought to a volume of 25 mL with CH_3CN.

RESULTS

Computational

Data, for the lowest energy conformations, of each individual species used for the calculation of BDEs is presented in Table I, including the total Born-Oppenheimer energies, the ZPEs, the isodesmic corrections and H_{corr} values (33). Higher energy confirmers are shown in Supplemental Table 1. The lowest energy conformations of each model, **M1**-**M4**, and their corresponding radical derivatives: Radical 1a (**R1a**), Radical 1b (**R1b**), Radical 2 (**R2**), Radical 3 (**R3**), Radical 4a (**R4a**) and Radical 4b (**R4b**) can be found in supplemental Figs. S1 and S2, respectively. As expected, due to conjugation and hyperconjugation, bonds alpha to the radical center are shorter in the radicals than in their parents. All radical centers are virtually planar except for **R3**, where the methyl group lies 20.3° out of the C(radical center)-O-H plane. This is due to the weak 3-electron bond interaction between the C-radical and oxygen. The final results at the B3LYP/6-311 + G(d,p)// B3LYP/6-31 + G(d) level of theory with isodesmic corrections are presented in Table I. The C-H^1 bond of **M1** has the lowest BDE with the benzylic hydrogen C-H^2 bond BDE of **M2** within 1 kcal mol^{-1} suggesting that these sites are the most likely sites for attack. The low BDE of C-H^1 is due to the apparent stability of the **R1** radical that benefits from resonance as well as possible captodative stabilization due to the adjacent pyrrole and carboxylic acid groups (33). The BDEs

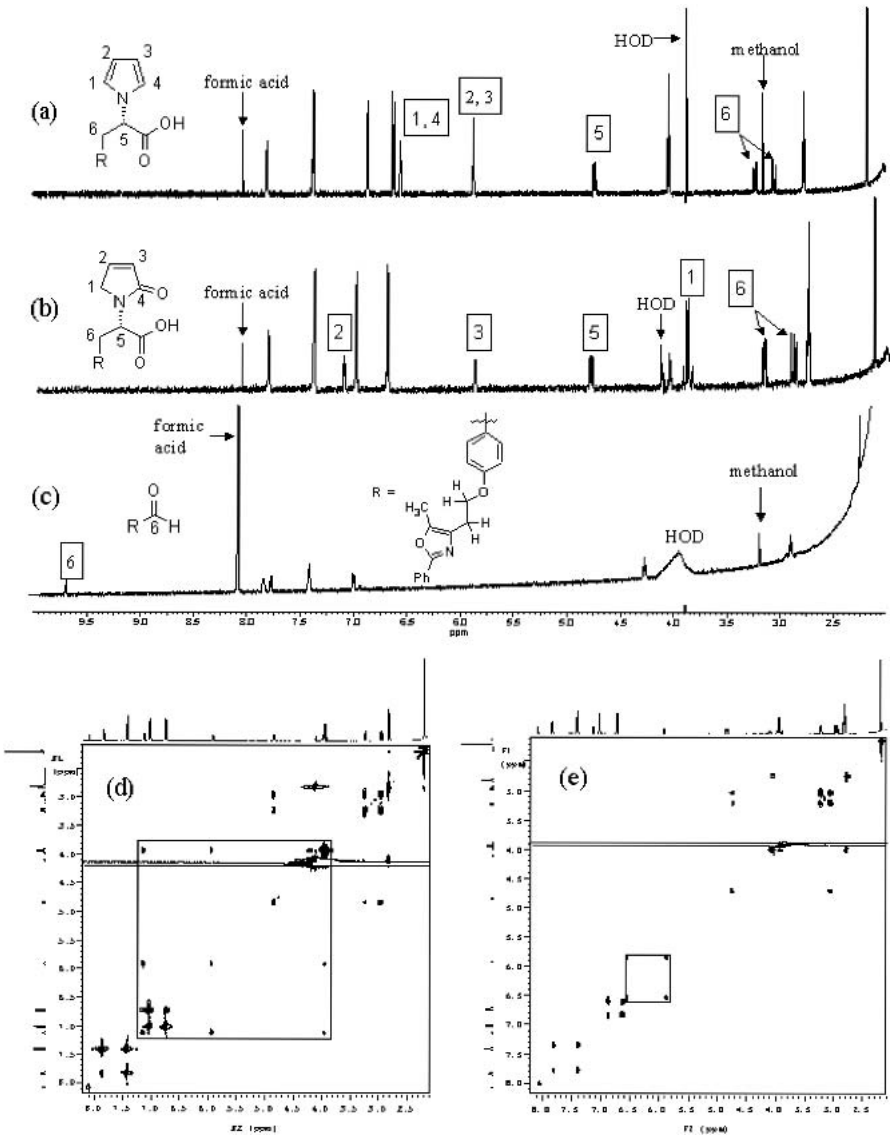

Fig. 7. ^{1}H-NMR spectra of (a) compound **1**; (b) degradant **2**; and (c) degradant **3** and TOCSY spectra of (d) compound **1** and (e) degradant **2**.

for **M1a** and **M1b** are identical, indicating no effect of deprotonating the acid. Figure 3 shows the HOMO of compound **1**, an overall bonding molecular orbital representing the π-system of the pyrrole ring. Therefore, FMO theory predicts that the pyrrole ring should be the site of peroxide attack and electron transfer.

Experimental

Under hydrogen peroxide stress conditions, desirable levels of degradation (20%) for both system suitability studies and product analysis were achieved after 10 days (Fig. 4a). One primary degradation product, **2**, is clearly observed, with a relative retention time (RRT) of 0.63, and a positive m/z of 433. Chromatographic results for the three sets of autoxidative conditions tested are shown in Fig. 4. The results for autoxidation of **1** on exposure to atmospheric oxygen and radical initiator at 60°C (Fig. 4b) clearly show the growth of a primary degradant, **3**, at a RRT of 0.74 and a positive m/z = 308. A secondary degradant with m/z = 433 was also observed and confirmed to be the same degradant, **2**, observed under H_2O_2 degradation conditions by comparison of the collision spectrum, RRT, and UV-vis spectrum. Under these conditions ~19% degradation was reached in 10 days. On exposure of **1** to pressurized oxygen without initiator at 60°C (Fig. 4c), and to pressurized oxygen with initiator at 60°C (Fig. 4d) the samples reached ~25% and ~32% degradation respectively by day 5 and ~52% degradation each by day 10. In both cases the day 5 samples give a level of degradation that would be suitable for analytical methodology development and degradant analysis. The results are very similar to those observed under atmospheric oxygen conditions (Fig. 4b) with **3** remaining as the primary degradant. It is clear, however, that the low level of degradation observed under the atmospheric oxygen conditions may be more meaningful with respect to ICH stability. The high level of degradation observed in the 10 day samples would not be suitable for either analytical method development or degradant analysis due to interference from secondary oxidative degradants whose mechanistic pathways would be very unlikely in an actual solid phase drug formulation.

The hydrogen peroxide results, Fig. 4(a), gave one primary degradation product with a RRT of 0.63 and the collision spectra shown in Fig. 5(b). Figure 5(b) has a parent m/z = 433 and shows two daughter ions: m/z = 387 and 186. Compound **1** has a parent mass of 416 g mol^{-1} so m/z = 433 suggests addition of one oxygen while the m/z = 186 daughter ion, which is also present in the collision spectra of **1** (Fig. 5a), indicates that the lower portion of the molecule remains unoxidized. This is in agreement with the computational FMO predictions. Pyrroles are in fact known to react with peroxides to form pyrrolinones (Fig. 6, path a) (34,35).

Oxidation of **1** under autoxidation conditions yielded a different primary degradant, **3**, with a relative retention time of 0.74 (Fig. 6b–6d). Figure 5(c) shows the LC/MS/MS collision spectra for this system. The parent ion for this system has a m/z = 308 and again shows a daughter ion of m/z = 186. This is consistent with the computational prediction that autoxidation will take place at the C-H^2 group or the C-H^1. The C-H^1 group was predicted to be the most reactive on the basis of BDEs but it was not possible to derive a direct mechanistic pathway to the m/z = 308 product. However, H-atom abstraction from the C-H^2 bond, predicted to have a BDE less than 1 kcal mol^{-1} higher in energy, leads directly to the observed product mass. The proposed mechanism also requires the participation of radical formation at the C-H^1 site (Fig. 6,

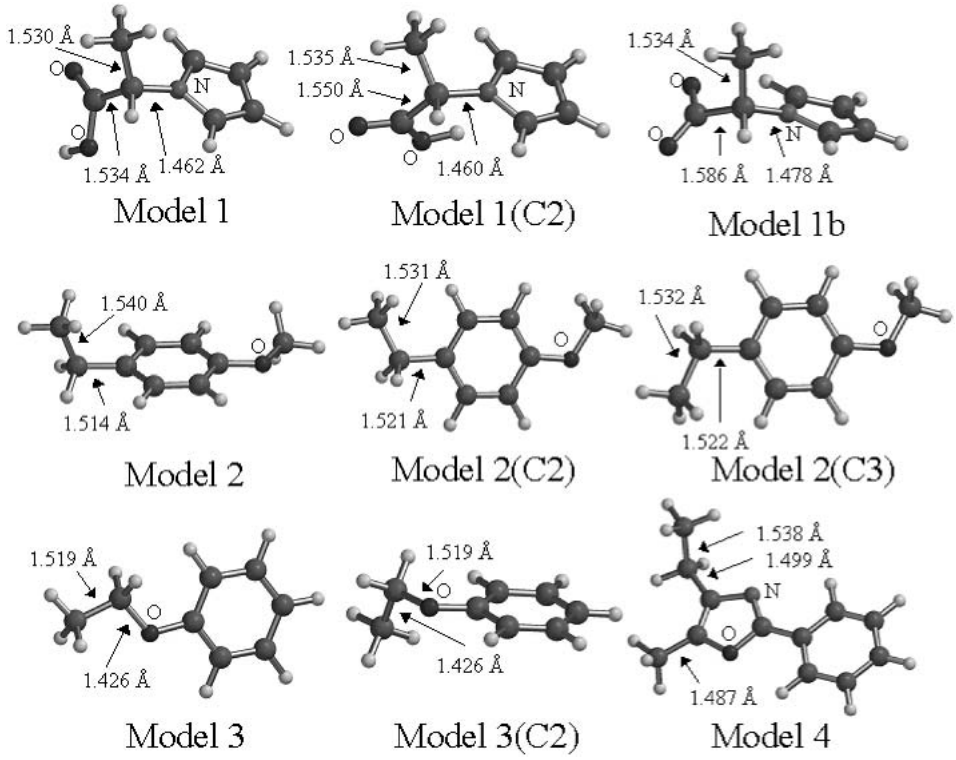

Fig. S1. Model Geometries and their higher energy conformations at the B3LYP/6-31G(d) level.

path b), with a structure that is very similar to **R1**, predicted be very stable by the computational results.

Attempts to isolate **2** failed so LC/MS/NMR was used for the final structural confirmation of both **2** and **3** (see Supplemental NMR Analysis). Analytical solutions of oxidized compound **1** were injected onto the LC/MS/NMR system described above. Retention times for the components of interest were 7.5 min, 14.8 min and 16 min for **2**, **3**, and **1**, respectively. Stop-flow proton LC/NMR spectra of **1**, **2**, and **3** are shown in Fig. 7. Comparison of the proton spectra of **1** (Fig. 7a) and **2** (Fig. 7b) indicates that forced degradation of the parent, **1**, under hydrogen peroxide stress conditions resulted in modification of the pyrrole portion of the molecule, while spectral features due to all other parts of the molecule are virtually identical for **1** and **2**. The spectrum of **2** is consistent with the indicated structure (36,37). A more detailed NMR analysis is included as supplemental information. Two-dimensional ^{1}H-^{1}H Total Correlation (TOCSY) spectra of **1** and **2** were acquired to confirm connectivity of coupled spin systems of the pyrrolinone ring (Fig. 7d and 7e). The TOCSY spectrum of **1** (Fig. 7d) shows that the two pairs of equivalent protons for the pyrrole ring (at 6.55 and 5.87 ppm) are coupled, while the TOCSY spectrum of **2** (Fig. 7e) shows that the three multiplets (7.13, 5.92, and 3.94 ppm) of the pyrrolinone ring are coupled. All other regions of the TOCSY spectra for **1** and **2** are equivalent, indicating that oxidation is confined to the pyrrole ring of the parent, and confirming the predicted structure.

The stop-flow proton LC/NMR spectrum of **3** is shown in Fig. 7(c). The most striking feature of this spectrum is the presence of a sharp singlet at 9.65 ppm that is indicative of an aldehyde. The remaining spectral features are consistent with the structure of **3**. There are several missing resonances of note, which confirm the identification of **3**. These include resonances associated with the pyrrole ring, a pair of diastereotopic protons at 3.0 ppm, and a doublet of doublets at 4.75 ppm corresponding to the proton attachment to carbon 6.

Analysis of the excipient blend showed that the excipients did promote oxidation of **1**. After 6 weeks, all of the standard drug blend samples showed formation of the m/z =

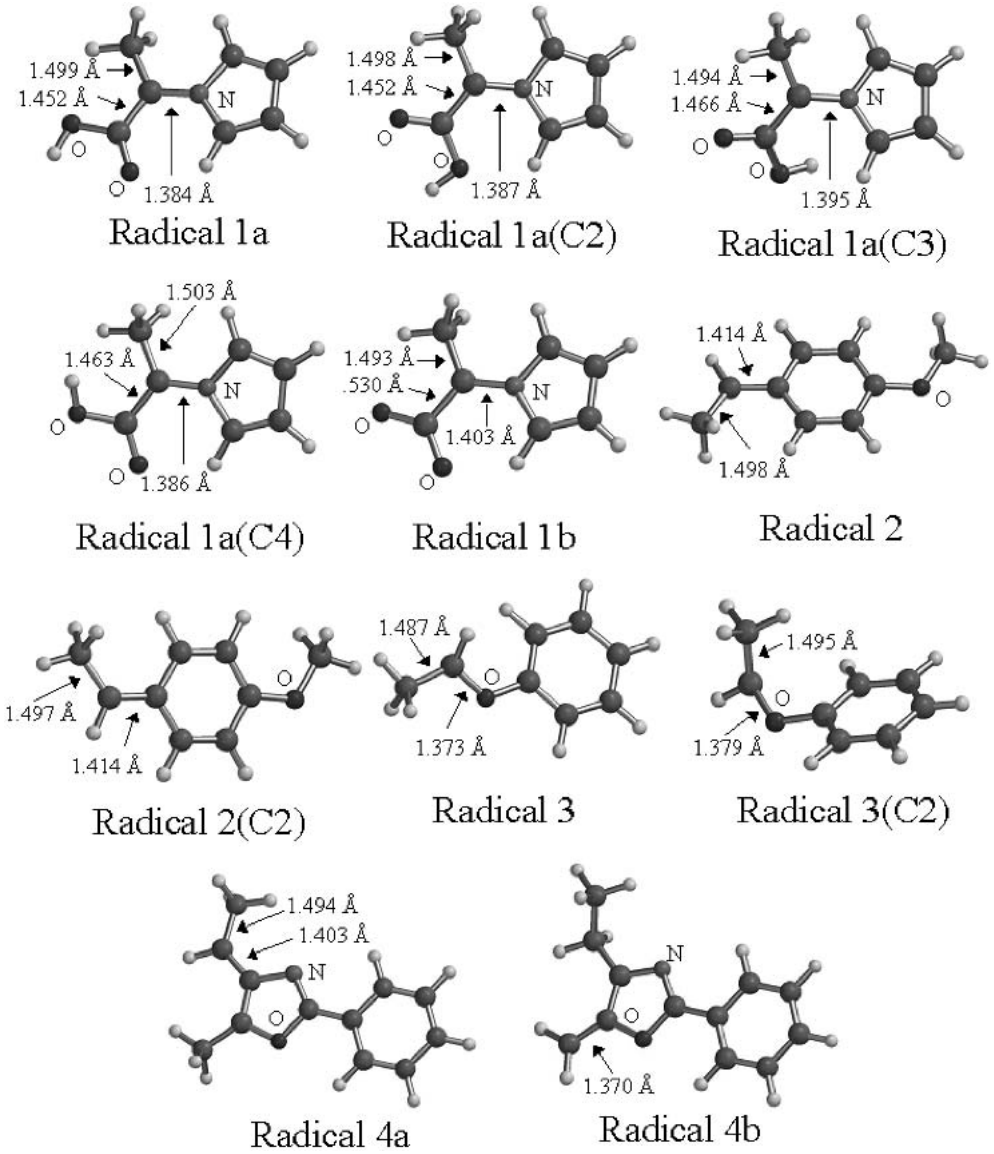

Fig. S2. Radical geometries and their higher energy conformations at the B3LYP/6-31G(d) level.

433 peroxide degradant, **2**, in the LC/MS scans. Likewise, in the pressurized O_2 at 60°C standard drug blend samples the autoxidized m/z = 308 degradant, **3**, was observed. Neither degradant could be detected in the benzyloxazol, **1**, samples, in the absence of excipients, under any of the conditions tested here. Formation of **2** may result from residual peroxide impurties in the excipients. The observation of the autoxidization product, **3**, in the pressurized O_2 at 60°C standard drug blend samples but not in the pure compound **1** control samples may be attributed to plasticization effects (6).

DISCUSSION

The purpose of forced degradation studies is 2-fold, testing the analytical method to ensure selectivity and understanding the stability of the active pharmaceutical ingredient. In order to fill these objectives it is important that the oxidative methods used are predictive of ICH stability. Not surprisingly the hydrogen peroxide and autoxidation methods used in this paper gave very different results, while our excipient blend yielded not only peroxide degradants but also autoxidation products. These results are consistent with Boccardi's, who compared oxidative degradation profiles under thermal, light, hydrogen peroxide, transition metals, and radical initiator conditions and found that the radical initiator, autoxidation conditions, most closely resembled oxidation of the model drugs under prolonged storage (38). This emphasizes the importance of including autoxidation as well as peroxide conditions in any forced degradation study designed for analytical method development. This is not the standard practice in the industry (1) but the results presented here suggest that including a set of autoxidative conditions need not imply an additional large expense or effort and can be implemented by the simple use of a radical initiator with atmospheric oxygen.

The primary focus of this work was to examine computational approaches, to complement oxidative forced degradation studies. A key step in this process would be the early identification of likely degradation products and pathways. Two computational methods were outlined that can be applied to typical active pharmaceutical ingredients. In the first of these approaches a simple FMO analysis was performed on the model compound **1** to identify the most likely reactive site for peroxides. The HOMO was generated at the HF/6-31G*//HF/3-21G* level of theory, calculations easily performed by any modern PC. The results indicated that the pyrrole ring should be the most susceptible π-system to peroxide oxidation and electron transfer. LC/MS/MS results of the hydrogen peroxide forced degradation study, indicated that the pyrrole ring did belong to the portion of the molecule that was being oxidized, allowing for the proposal of **2** as the likely degradant. In the second computational approach calculated C-H BDEs were used to predict likely autoxidation pathways based on the fact that hydrogen atom abstraction is one of the key initiating steps in these reactions. The BDEs were calculated at the B3LYP/6-311 + G**// B3LYP/6-31G* level with isodesmic corrections, calculations also well within the reach of modern personal computers. During autoxidation, peroxyl radicals ($ROO^{\bullet}$) are the key intermediate responsible for propagating the reaction by H-atom abstraction from API. Therefore, in order for the propagation step to be favorable, the BDE of the R-H bond being attacked should be less than that of an alkyl peroxide (ROO-H), ~90 kcal/mol (7). Table I indicates that the $C\text{-}H^1$, $C\text{-}H^2$ and $C\text{-}H^{4a}$ bonds all meet this criterion while the $C\text{-}H^1$ and $C\text{-}H^2$ are within 1 kcal mol^{-1} of each other and are predicted to be the most labile sites. The forced degradation studies for compound **1** confirmed that this portion of the molecule was degraded, allowing structure **3** to be proposed as the most likely degradant. Having the proposed degradant structures afforded fast and easy structural confirmation by LC/MS/NMR, a task which would have been much more difficult otherwise.

Supplemental NMR Analysis of 2

Comparison of the proton spectra of **1** (Fig. 7a) and **2** (Fig. 7b) indicates that modification of the pyrrole portion of the molecule, while spectral features due to all other parts of the molecule are virtually identical. The spectrum of **2** is consistent with the indicated structure (37,38). The loss of a multiplet (integral = 2 protons) at 6.55 ppm and the concomitant appearance of a multiplet centered at 3.94 ppm (integral = 2 protons) confirms the loss of one double bond in the pyrrole ring. The newly observed multiplet at 7.13 ppm is consistent with the presence of a highly deshielded proton in a conjugated system comprised of carbons 2, 3, 4, and the oxygen attached to carbon 4. The integral for the multiplet at 5.87 ppm in the spectrum for **1** is double the integral of the mul-

Supplemental Table I. Total Energies and Zero Point Corrections for All Model and Radical Conformations at the B3LYP/6-31G(d) Level of Theory

Species	Energy hartrees	ZPE kcal mol^{-1}
Stable Species		
Toluene	–271.566690	78.95
Propylene	–117.907543	49.22
Methanol	–115.714408	31.68
Glycine	–284.423448	49.28
Model 1a	–477.355822	94.88
Model 1a (C2)	–477.352598	94.79
Model 1b	–476.798211	86.54
Model 2	–425.402468	117.08
Model 2 (C2)	–425.400754	116.96
Model 2 (C3)	–425.400498	117.02
Model 3	–386.090671	99.75
Model 3 (C2)	–386.088304	99.77
Model 4	–595.095924	138.13
Radicals		
$^{\bullet}H$	–0.500273	0.00
$^{\bullet}CH_2Ph$	–270.915156	70.65
$^{\bullet}CH_2CH=CH_2$	–117.260374	40.82
$^{\bullet}CH_2OH$	–115.052037	23.08
*C-glycine radical	–283.790367	41.21
Radical 1a	–476.720866	85.33
Radical 1a (C2)	–476.718690	87.03
Radical 1a (C3)	–476.709618	86.74
Radical 1a (C4)	–476.707166	86.76
Radical 1b	–476.155478	78.34
Radical 2	–424.756192	108.14
Radical 2 (C2)	–424.756322	108.31
Radical 3	–385.430208	90.92
Radical 3 (C2)	–385.426307	90.97
Radical 4a	–594.449597	129.41
Radical 4b	–594.452016	129.78

*

tiplet in the spectrum of **2,** indicating the loss of one of the two original equivalent protons. Two-dimensional ^1H-^1H Total Correlation (TOCSY) spectra using WET solvent suppression were acquired to confirm connectivity of coupled spin systems. The TOCSY spectra of **1** and **2** are shown in Fig. 9d, 9e. The TOCSY spectrum of **1** (Fig. 9d) shows two pairs of equivalent protons for the pyrrole ring (at 6.55 and 5.87 ppm), while the TOCSY spectrum of **2** (Fig. 9e) shows the three multiplets (7.13, 5.92, and 3.94 ppm) of the pyrrolinone ring are coupled. All other regions of the TOCSY spectra for **1** and **2** are equivalent, indicating that oxidation is confined to the pyrrole ring of the parent and confirming the predicted structure.

ACKNOWLEDGMENTS

The authors wish to thank Anita L. Freed, Karen M. Alsante, Brian Tobias, Tim Hurley, David L. Pole, and Kevin Kolodsick, of Pfizer Inc.; David Rossi, of Mylan Pharmaceuticals, Inc.; as well as Arvi Rauk and David A. Armstrong of the University of Calgary for helpful discussions. D.L.R. thanks Pfizer Inc. for a postdoctoral research fellowship.

REFERENCES

1. K. A. Alsante, L. Martin, and S. W. Baertschi. A stress testing benchmarking study. *Pharm. Tech.* **2**:60–72 (2003).
2. PP. Crowley and L. Martini. Drug-EXCIPIENT INTERACTIONS. *Pharm. Technol. Eur.* **13**:26–34 (2001).
3. K. A. Alsante and T. Hatajik. Purposeful Degradation Best Practice Guidance Document for Exploratory Development Compounds, *internal document*, Pfizer Inc., Degradation Resource Group (1999).
4. I. C. H. Harmonized Tripartite Guidline. Stability Testing of New Drug Substances and Products, U.S. Department of Health and Human Services Food and Drug Administration (CDER) Nov. 2003 r2.
5. Guidance for Industry. Q1A Stability Testing of New Drug Substances and Products, U.S. Department of Health and Human Services, Food and Drug Adminstration, Center for Drug Evaluation and Research (CDER), Center for Biologics Evaluation and Research (CBER), ICH, August 2001, Recision 1. http://www.fda.gov/cder/guidance/index.htm.
6. K. C. Waterman, R. C. Adami, K. A. Alsante, J. Hong, M. S. Landis, F. Lombardo, and C. J. Roberts. Stablization of pharmaceuticals to oxidative degradation. *Pharm. Develop. Tech.* **7**:1–32 (2002).
7. S. W. Hovorka and C. Schöniech. Oxidative degradation of pharmaceuuticals: theory, mechanisms and inhibition. *J. Pharm. Sci.* **90**:253–269 (2001).
8. P. Gamache, R. McCarthy, J. Waraska, and I. Acworth. Pharmaceutical oxidative stability profiling with high-throughput voltammetry. *Am. Lab.* **6**:21–25 (2003).
9. Arvi Rauk. *Orbital Interaction Theory of Organic Chemistry*, 2nd ed., John Wiley & Sons, New York, 2001.
10. C. von Sonntag. *The Chemical Basis of Radiation Biology,* Taylor and Francis, London, 1987.
11. G. S. Hammond. A correlation of reaction rates. *J. Am. Chem. Soc.* **77**:334–338 (1955).
12. M. Jonsson, D. D. M. Wayner, D. A. Armstrong, D. Yu, and A. Rauk. On the thermodynamics of peptide oxidation: anhydrides of glycine and alanine, *J. Chem. Soc. Perkin Trans.* **2**:1967–1972 (1998).
13. K. G. Liu, M. H. Lambert, A. H. Ayscue, B. R. Henke, L. M. Leenitzer, W. R. Oliver Jr., K. D. Plunket, H. E. Xu, D. D. Sternbach, and T. M. Willson. Synthesis and biological activity of L-tyrosine-based PPARγ agonists with reduced molecular weight. *Bioorg. Med. Chem. Lett.* **11**:3111–3113 (2001).
14. *Spartan'02*, Wavefunction, Inc., Irvine, CA.
15. A. P. Scott and L. Radom. Harmonic vibrational frequencies: an evaluation of hartree-fock, møller-plesset, quadratic configuration interaction, density functional theory, and semiempirical scale factors. *J. Phys. Chem.* **100**:16502–16513 (1996).
16. N. Kobko and J. J. Dannenberg. Effect of basis set superposition error (BSSE) upon ab initio calculations of organic transition states. *J. Phys. Chem. A* **105**:1944–1950 (2001).
17. W. J. Hehre, R. Ditchfield, L. Radom, and J. A. Pople. Molecular orbital theory of the electronic structure of organic compounds. V. Molecular theory of bond separation. *J. Am. Chem. Soc.* **92**: 4796–4816 (1970).
18. D. A. Armstrong, D. Yu, and A. Rauk. Oxidative damage to the glycyl α-carbon site in proteins: an ab initio study of the C-H bond dissociation energy and the reduction potential of the C-centered radical. *Can. J. Chem.* **74**:1192–1199 (1996).
19. M. Jonsson, D. M. Wayner, D. A. Armstrong, D. Yu, and A. Rauk. On the thermodynamics of peptide oxidation: anhydrides of glycine and alanine, *J. Chem. Soc. Perkin Trans.* **2**:1967–1972 (1998).
20. E. J. Prosen, R. Gilmont, and F. D. Rossini. Heats of combustion of benzene, toluene, ethyl-benzene, o-xylene, m-xylene, p-xylene, n-propylbenzene, and styrene. *J. Res. NBS* **34**:65–70 (1945).
21. S. Soonho, D. M. Golden, R. K. Hanson, and C. T. Bowman. A shock tube study of benzylamine decomposition: overall rate coefficient and heat of formation of the benzyl radical. *J. Phys. Chem. A* **106**:6094–6098 (2002).
22. J. D. Cox, D. D. Wagman, and V. A. Medvedev. CODATA Key Values for Thermodynamics, Hemisphere Publishing Corp., New York, 1984, p. 1.
23. S. Furuyama, D. M. Golden, and S. W. Benson. Thermochemistry of the gas phase equilibria i-C_3H_7I = C_3H_6 + HI, n-C_3H_7I = i-C_3H_7I, and C_3H_6 + 2HI = C_3H_8 + I_2. *J. Chem. Thermodyn.* **1**:363–375 (1969).
24. J. R. Lacher, C. H. Walden, K. R. Lea, and J. D. Park. Vapor phase heats of hydrobromination of cyclopropane and propylene. *J. Am. Chem. Soc.* **72**:331–333 (1950).
25. W. Tsang. Heats of formation of organic free radicals by kinetic methods in Energetics of Organic Free Radicals, J. A. Martinho Simoes, A. Greenberg, J. F. Liebman, Blackie Academic and Professional, London, 1996, pp. 22–58.
26. J. Hine and K. Arata. Keto-Enol tautomerism. II. The calorimetrical determination of the equilibrium constants for keto-enol tautomerism for cyclohexanone. *Bull. Chem. Soc. Jpn.* **49**:3089–3092 (1976).
27. J. H. S. Green, Revision of the values of the heats of formation of normal alcohols, *Chem. Ind. (London)* 1215–1216 (1960).
28. D. A. Block, D. A. Armstrong, and A. Rauk. Gas phase free energies of formation and free energies of solution of C-centered free radicals from alcohols: a quantum mechanical-Monte Carlo study. *J. Phys. Chem. A* **103**:3562–3568 (1999).
29. D. A. McQuarrie. *Statistical Thermodynamics*; Harper & Row: New York, NY, 1973.
30. J. W. Ochterski. Thermochemistry in Gaussian ©2000 Technical paper, Gaussian, Inc. help@gaussian.com
31. S. Smallcombe, S. Patt, and P. Keifer. WET solvent suppression and its applications to LC NMR and high-resolution NMR spectroscopy. *J. Magn. Reson. A* **117**:295–303 (1995).
32. P. Crowley and L. Martini. Drug-excipient interactions. *Pharm. Technol. Eur.* **13**:26–34 (2001).
33. F. G. Bordwell, X. M. Zhang, and M. S. Alnajjar. Effects of adjacent acceptors and donors on the stabilities of carbon-centered radicals. *J. Am. Chem. Soc.* **114**:7623–7629 (1992).
34. R. A. Jones and G. P. Bean. *The Chemistry of Pyrroles*. Academic Press. *New York* **34**:209–247 (1977).
35. A. Gossauer and P. Nesvadba. Reactivity of the 1H-pyrrole ring system. Oxidation and reduction of the pyrrole ring. In *Chemistry of Heterocyclic Compounds, Pyrroles, Pt. 1*, Chichester. *United Kingdom* **48**:499–536 (1990).
36. J. Bordner and H. Rapoport. Synthesis of 2,2'-bipyrroles from 2-pyrrolinones. *J. Org. Chem.* **30**:3824–3828 (1965).
37. E. B. Smith and H. B. Jensen. Autoxidation of three 1-alkylpyrroles. *J. Org. Chem.* **32**:3330–3334 (1967).
38. G. Boccardi. Autoxidation of drugs: prediction of degradation impurties from results of reaction with radical chain initiators. *Farmaco* **49**:431–435 (1994).